

Matthieu J.B. Cartigny and George Postma

---

## Abstract

Turbidity currents in the submarine seascape are what river flows are in terrestrial landscapes. While rivers transport sediment from the mountains through valleys towards the sea, turbidity currents transport sediment from the shallow marine realms through canyons towards the deeper abyssal plains. The large scale architecture of both systems is remarkably similar. Yet, there are some fundamental differences between rivers and turbidity currents, the most fundamental one being their density difference; the density of river water is thousand times denser than its surrounding air, while the density of a turbidity current can never be more than twice as dense as its ambient water. In addition, rivers do not depend on their sediment load to flow, while turbidity (density) currents do need the sediment derived excess density to flow. These physical differences change their morphodynamics on the bedform scale. Present day high-resolution seafloor observations show that turbidity current path ways are covered with bedforms that are fundamentally different from those that occur in river channels. In this chapter we point out these differences and present a 3D bedform stability diagram for turbidites.

---

## Keywords

Bedforms • Bedform stability diagram • Turbidity currents • Antidunes • Cyclic steps

---

## 6.1 Turbidity Current Bedforms

Compared with the well-studied range of bedforms occurring in river systems, very little is known about the equivalent range of bedforms that are observed in turbidity current systems. Most of our present day knowledge of turbidity current bedforms is derived from seafloor surveys (e.g. Normark et al. 1980; Migeon et al. 2001; Zhong et al. 2015) and from studies of bedforms preserved in the geological record through outcrop studies (e.g. Walker 1967; Skipper 1971; Mutti 1992; Postma et al. 2014; Ventra et al. 2015).

---

M.J.B. Cartigny (✉)  
National Oceanography Centre, University of Southampton  
Waterfront Campus, Southampton, UK  
e-mail: m.cartigny@noc.ac.uk

G. Postma  
Faculty of Geosciences, Utrecht University,  
Utrecht, The Netherlands

Recent years have seen an advance in bedform knowledge due to upcoming high-resolution seafloor surveys with Autonomous Underwater Vehicles (i.e. Paull et al. 2011) and detailed short-period-repeat mapping of turbidity current systems (i.e. Hughes Clarke et al. 2012). These studies have shown that turbidity current bedforms are typically long and characterized by low stoss- and leeside inclinations, while their crests migrate against the flow direction. Their dynamic morphology is thus in great contrast to river bedforms, such as dunes, which have steep lee-sides and typically migrate down-current. Given that the seafloor sediments are similar to those in river beds, any of these differences must be related to physical differences between river and turbidity currents associated with their dynamic interaction with the bed.

The main physical difference between river flow and a turbidity current is centred on their difference in relative density. The excess density of turbidity currents, in relation

to the ambient sea water, is formed by the amount of sediment that it is carrying, which limits the density of the flow to a maximum of twice that of its surrounding water. This is in contrast with the excess density of river water, which is around a thousand times heavier than the surrounding air and thereby relatively insensitive to the extra weight of suspended sediment.

The low relative density of turbidity currents impact their morphodynamics in two ways. Firstly, waves propagating on the top of the flow are slowed down, as these are driven by gravity which in turbidity current is strongly reduced due to buoyancy forces. Early experimental bedform work of Guy et al. (1966) has shown that currents with velocities below the surface wave propagation velocity results in a range of down-current migrating bedforms, like ripples and dunes. In contrast, currents with flow velocities ( $U_{flow}$ ) that exceed the wave propagation velocity ( $U_{wave}$ ) lead to up-current migration bedforms, such as antidunes and cyclic steps (Taki and Parker 2005). The ratio of flow velocity over wave propagation velocity is expressed by the densimetric Froude number

( $Fr' = U_{flow}/U_{wave} = U_{flow}/\sqrt{(\rho_{flow} - \rho_w)gH/\rho_{flow}}$ ), where  $\rho_{flow}$ ,  $\rho_w$  are the densities of the flow and the water, respectively,  $g$  the acceleration of gravity and  $H$  is the flow depth. Supercritical flows have a flow velocity that exceeds the wave propagation velocity ( $Fr' > 1$ ) while for subcritical flows the opposite holds. Prevailing supercritical conditions in turbidity currents are confirmed by: (1) direct measurements of turbidity currents (Xu 2010), (2) experimental and numerical modelling (Middleton 1966; Hand 1974; Kostic and Parker 2006), (3) monitoring up-current migrating bedforms (Migeon et al. 2001; Smith et al. 2005; Hughes Clarke et al. 2012), and (4) observations of supercritical-flow bedforms in successions of turbidity current deposits in the rock record (Walker 1967; Skipper 1971; Postma et al. 2014; Ventra et al. 2015).

Secondly, the direct connection between the sediment-based relative density and the flow velocity make turbidity currents far more unstable than river flows. If turbidity currents entrain more sediment, their driving force goes up, which in turn speeds up the flow and further enhances sediment entrainment (so called auto-ignition, Parker et al. 1986). Running the same cycle in the opposite direction (waning flow) leads to positively enforced loops of deceleration and sediment fall-out. In such waning flow conditions sediment collects in high concentrations at the base of the flow before slowly coming to a complete standstill (Postma et al. 1988; Sohn 1997; Cartigny et al. 2013; Sumner and Paull 2014). Such dense basal layers will have their own densimetric Froude numbers, as waves are often seen to form on the top interface of dense basal layers (Cartigny et al. 2013; Sumner and Paull 2014). This has led

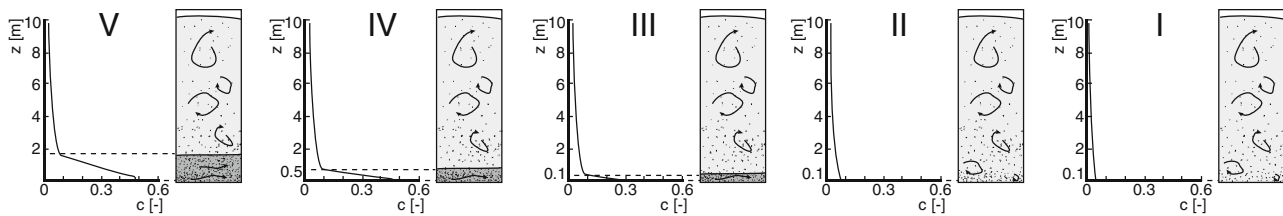
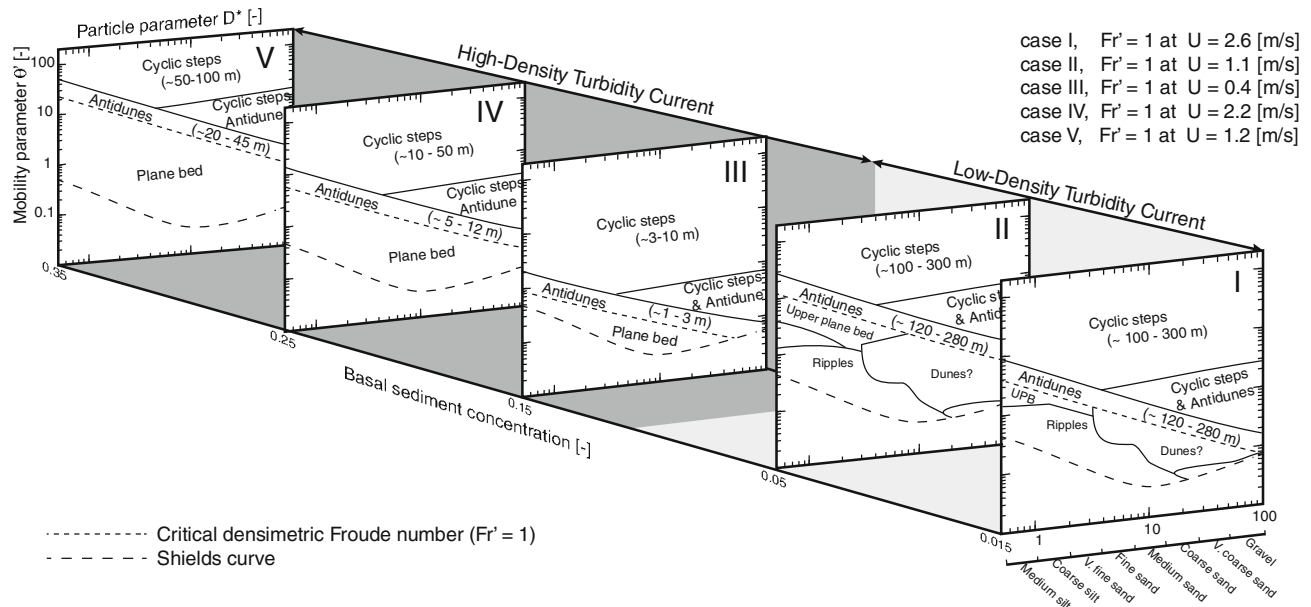
to the idea that dense basal layers will have their own bedform dynamics that is largely independent of the main flow (Postma et al. 2009; Postma and Cartigny 2014). Such dense basal layer bedforms are only thought to form under supercritical-flow conditions, as all subcritical bedform are dependent on turbulence, which is severely suppressed in dense basal layers. Dense basal layers flowing subcritically are thought to form long stretches of virtually flat basin floor (Postma and Cartigny 2014). In the rock record these deposits are characterized by centimetre-thick planar laminations of spaced and crude laminations (Hiscott 1994; Talling et al. 2012), which are thought to reflect the high basal sediment concentrations (Cartigny et al. 2013).

## 6.2 Bedform Stability Diagram for Turbidity Currents

The tendencies of turbidity currents to be supercritical and to form dense basal layers are now taken into account and introduced in a bedform stability diagram originally developed for river flows (Cartigny et al. 2014). Five examples of turbidity currents with increasing basal sediment concentrations, will now be discussed in more detail.

In panel I of Fig. 6.1b the bedform stability diagram is drawn for a dilute, 10 m thick turbidity current without a dense basal layer. The vertical concentration profile and turbulence characteristics are indicated for each panel in Fig. 6.1a. On the horizontal axes there is a dimensionless grain size, called particle parameter,  $D^* = D[(\rho_s - \rho_w)g/(\rho_w \nu^2)]^{1/3}$ , where  $D$  is the particle diameter,  $\rho_s$  is the density of the sediment and  $\nu$  is the viscosity of the water. On the vertical axes there is a dimensionless shear stress, called mobility parameter,  $\theta' = \rho_w U^2 / [(\rho_s - \rho_w) C'^2 D]$ , where  $C'$  is the Chezy parameter ( $C' = 18 \log(1.25H/D)$ ), see Cartigny et al. (2014) for more details on these parameters. The vertical position on this panel and thereby the type of bedform that will develop is determined by the bed shear stress, which is dominantly controlled by the flow velocity. If the mobility parameter drops below the Shields curve, then the bed shear stresses are no longer sufficient to transport sediment and bedforms will not develop (Shields 1936). The critical densimetric Froude line separates the subcritical bedforms such as ripples and dunes (Guy et al. 1966) from supercritical bedforms such as antidunes and cyclic steps (Cartigny et al. 2014). The indicated length scale of the antidunes is calculated using the work of Hand (1974) and that of the cyclic step is based on numerical simulations of Kostic (2011), Cartigny et al. (2011).

Panel II in Fig. 6.1b shows the case for a slightly higher basal sediment concentration, as indicated on the third axes of the bedform stability diagram, but still lacks a clear basal

**(a)** Five sediment concentration profiles for a turbidity current 10 [m] thick**(b)** Bedform stability diagram associated with the five cases shown in a**Fig. 6.1** **a** Five 10-m thick turbidity currents with different concentration profiles and resulting dense basal layers; **b** bedform stability diagrams associated with the five flow stratification types depicted in **a** (modified from Cartigny 2012)

density stratification. The stability diagram is very similar to that of case I, but the  $Fr' = 1$  line has shifted upwards as a result of the increased sediment concentration.

Panel III is similar to case II, but now bedform formation is governed by a thin dense basal layer (0.1 m) at the base of the flow, which buffers the bed from the dilute overriding flow. Its limited thickness makes it prone to supercritical flow and causes the downward expansion of the supercritical flow domain in the diagram. Furthermore, the high sediment concentrations near the base of the flow are now thought to suppress the turbulence and thereby preventing the formation of any ripples and dunes.

Panel IV is characterized by a thicker (0.5 m) dense basal layer, as in case III, its thickness making it less prone to supercritical flow, thereby shifting the supercritical flow domain back up again in the diagram.

Panel V shows a very thick (2 m), dense basal layer, which again shifts the supercritical flow field further upwards.

### 6.3 Discussion

As only a few experimental and numerical studies have been done on turbidity current bedforms (Hand 1974; Kostic and Parker 2006; Spinewine et al. 2009; Sequeiros et al. 2010), it is emphasised that the bedform stability diagram presented here is based on many assumptions, and should be seen as a first attempt to estimate the impact of differences in flow dynamics of rivers and turbidity currents on bedform formation.

Although the existence of denser basal layers in turbidity currents is now becoming more widely accepted after they were directly observed from a submersible caught in a turbidity current (Sumner and Paull 2014), the morphodynamics of these basal layers still remains virtually unstudied. Here we assume that a dense basal layer is able to form supercritical bedforms such as antidunes and cyclic steps, as flow instabilities and their associated processes, like standing waves and hydraulic jumps, do not require a specific turbulence structure (Karcz and Kersey 1980; Weirich 1988).

Furthermore, turbidity currents are also likely to carry considerable amounts of clay in suspension, which have a profound effect on their morphodynamics, as demonstrated by experimental studies (Wan et al. 1994; Baas and Best 2008; Baas et al. 2009). These studies suggested that any bedform stability diagram for turbidity currents should also have a fourth dimension, in particular if the amount of transported clay is more than 6 % (see Baas et al. 2009).

The last limitation mentioned here is that the diagram as presented here is only intended for flows that are 10 m thick. Smaller or larger flow depth will have an impact on the position of the line representing critical densimetric Froude numbers, and hence for larger flows the supercritical-flow bedforms will move up in the diagram, while the opposite holds for thinner flows.

## References

- Baas, J.H. and Best, J.L. (2008). The dynamics of turbulent, transitional and laminar clay-laden flow over a fixed current ripple: *Sedimentology*, v. 55, p. 635–666.
- Baas, J.H., Best, J.L., Peakall, J., and Wang, M. (2009). A phase diagram for turbulent transitional and laminar clay suspension flows: *Journal of Sedimentary Research*, v. 79, p. 162–183.
- Cartigny, M.J.B. (2012). Morphodynamics of supercritical high-density turbidity currents. *Utrecht Studies in Earth Sciences*, PhD thesis, 153 pp.
- Cartigny, M.J.B., Postma, G., Van Den Berg, J.H. and Mastbergen D. R. (2011). A comparative study of sediment waves and cyclic steps based on geometries, internal structures and numerical modeling. *Mar. Geol.*, 280, 40–56.
- Cartigny, M.J.B., Eggenhuisen, J.T., Hansen, E.W.M. and Postma, G. (2013). Concentration-dependent flow stratification in experimental high-density turbidity currents and their relevance to turbidite facies models. *Journal of Sedimentary Research*, 83, 1046–1064, doi:10.2110/jsr.2013.71.
- Cartigny, M.J.B., Ventra D., Postma, G. and Van Den Berg, J.H. (2014). Morphodynamics and internal structures of bedforms under supercritical-flow conditions. *Sedimentology*, doi:10.1111/sed.12076.
- Guy, H. P., Simons, D. B., & Richardson, E. V. (1966). Summary of alluvial channel data from flume experiments, 1956–61 (No. 462-I).
- Hand, B.M. (1974). Supercritical flow in density currents. *J. Sed. Res.*, 44(3), 637–648.
- Hiscott, R. N. (1994). Traction-carpet stratification in turbidites—fact or fiction?. *Journal of Sedimentary Research*, 64(2).
- Hughes Clarke, J.E., Brucker, S., Muggah, J., Hamilton, T., Cartwright, D., Church, I. and Kuus, P. (2012). Temporal progression and spatial extent of mass wasting events on the Squamish prodelta slope, in Eberhardt, E., et al., eds., *Landslides and engineered slopes: Protecting society through improved understanding*: London, Taylor & Francis Group, p. 1091–1096.
- Karcz, I. and Kersey, D. (1980). Experimental study of free-surface flow instability and bedforms in shallow flows. *Sedimentary Geology*, 27(4), 263–300.
- Kostic, S. (2011). Modeling of submarine cyclic steps: Controls on their formation, migration, and architecture. *Geosphere*, 7(2), 294–304.
- Kostic, S. and Parker, G. (2006). The response of turbidity currents to a canyon–fan transition: internal hydraulic jumps and depositional signatures. *Journal of Hydraulic Research*, 44(5), 631–653.
- Middleton, G. V. (1966). Experiments on density and turbidity currents: II. Uniform flow of density currents. *Canadian Journal of Earth Sciences*, 3(5), 627–637.
- Migeon, S., Savoye, B., Zanella, E., Mulder, T., Faugères, J.C. and Weber, O. (2001). Detailed seismic-reflection and sedimentary study of turbidite sediment waves on the Var sedimentary ridge (SE France): Significance for sediment transport and deposition and for the mechanisms of sediment-wave construction: *Marine and Petroleum Geology*, v. 18, p. 179–208, doi:10.1016/S0264-8172(00)00060-X.
- Normark, W. R., Hess, G. R., Stow, D. A. V. and Bowen, A. J. (1980). Sediment waves on the Monterey Fan levee: a preliminary physical interpretation. *Marine Geology*, 37(1), 1–18.
- Mutti, E. (1992). Turbidite Sandstones. Agip Spec. Publ, Instituto de geologia, Univ. di Parma, Agip sp. A. 275 pp.
- Parker, G., Fukushima, Y. and Pantin, H. M. (1986). Self-accelerating turbidity currents. *Journal of Fluid Mechanics*, 171, 145–181.
- Paull, C. K., Caress, D. W., Ussler, W., Lundsten, E., and Meiner-Johnson, M. (2011). High-resolution bathymetry of the axial channels within Monterey and Soquel submarine canyons, offshore central California. *Geosphere*, 7, 1077–1101.
- Postma, G. and Cartigny, M. (2014). Supercritical and subcritical turbidity currents and their deposits- A synthesis, *Geology* 42, 987–990.
- Postma, G., Nemeč, W., and Kleinspehn, K. L. (1988). Large floating clasts in turbidites: a mechanism for their emplacement. *Sed. Geol.*, 58, 47–61.
- Postma, G., Cartigny, M. and Kleverlaan, K. (2009). Structureless, coarse-tail graded Bouma Ta formed by internal hydraulic jump of the turbidity current? *Sedimentary Geology* 219, 1–6.
- Postma, G., Kleverlaan, K. and Cartigny, M. (2014). Recognition of cyclic steps in sandy and gravelly turbidite sequences and consequences for the Bouma facies model. *Sedimentology* 61: 2268–2290, DOI:10.1111/sed.12135.
- Shields, A. (1936). *Anwendung der Aehnlichkeitsmechanik und der Turbulenzforschung auf die Geschiebebewegung*. Preussischen Versuchsanstalt für Wasserbau.
- Skipper, K. (1971). Antidune cross-stratification in a turbidite sequence, Cloridorme Formation, Gaspé, Québec. *Sedimentology*, 17(1-2), 51–68.
- Smith, D. P., Ruiz, G., Kvittek, R. and Iampietro, P. J. (2005). Semiannual patterns of erosion and deposition in upper Monterey Canyon from serial multibeam bathymetry. *Geological Society of America Bulletin*, 117(9–10), 1123–1133.
- Sohn, Y.K. (1997). On traction-carpet sedimentation. *J. Sed. Res.*, 67 (3), 502–509. Southard and Boguchwal 1990.
- Spinewine, B., Sequeiros, O. E., Garcia, M. H., Beaubouef, R. T., Sun, T., Savoye, B. and Parker, G. (2009). Experiments on wedge-shaped deep sea sedimentary deposits in minibasins and/or on channel levees emplaced by turbidity currents. Part II. Morphodynamic evolution of the wedge and of the associated bedforms. *Journal of Sedimentary Research*, 79(8), 608–628.
- Sequeiros, O. E., Spinewine, B., Beaubouef, R. T., Sun, T., Garcia, M. H. and Parker, G. (2010). Characteristics of velocity and excess density profiles of saline underflows and turbidity currents flowing over a mobile bed. *Journal of Hydraulic Engineering*, 136(7), 412–433.
- Sumner, E. J. and Paull, C. K. (2014). Swept away by a turbidity current in Mendocino submarine canyon, California. *Geophysical Research Letters*, 41(21), 7611–7618.
- Talling, P. J., Masson, D. G., Sumner, E. J. and Malgesini, G. (2012). Subaqueous sediment density flows: Depositional processes and deposit types. *Sedimentology*, 59(7), 1937–2003.
- Taki, K. and Parker, G. (2005). Transportational cyclic steps created by flow over an erodible bed. Part I. Experiments. *Journal of Hydraulic Research*, 43(5), 488–501.

- Ventra, D., Cartigny, M.J.B., Bijkerk, J. & Acikalin, S. (2015). Supercritical-flow structures on a Late Carboniferous delta front: sedimentologic and paleoclimatic significance. *Geology*. in press.
- Walker, R. G. (1967). Upper flow regime bed forms in turbidites of the Hatch Formation, Devonian of New York State. *Journal of Sedimentary Research*, 37(4).
- Wan, Z., Wang, Z. and Julien, P. Y. (1994). Hyperconcentrated flow. *Journal of Hydraulic Engineering*, 120(10), 1234–1234.
- Weirich, F. H. (1988). Field evidence for hydraulic jumps in subaqueous sediment gravity flows. *Nature*, 332, 626–629.
- Xu, J. P. (2010). Normalized velocity profiles of field-measured turbidity currents. *Geology*, 38(6), 563–566.
- Zhong, G., Cartigny, M. J., Kuang, Z. and Wang, L. (2015). Cyclic steps along the South Taiwan Shoal and West Penghu submarine canyons on the northeastern continental slope of the South China Sea. *Geological Society of America Bulletin*, 127(5–6), 804–824.